Atom Indonesia

Journal homepage: http://atomindonesia.brin.go.id

Core and/or No-Core Shell Model Calculations of the Nuclear Structure for the ^{6}Li, ^{32}S, ^{92}Mo, and ^{90}Zr Nuclei

A. A. Mohaimeed[1*], S. R. Sahib[2]

[1]Directorate of Education Babylon, Ministry of Education, Hillah, Iraq
[2]Directorate General of Education in Karbala Province, Ministry of Education, Karbala, Iraq

ARTICLE INFO

Article history:
Received 3 March 2025
Received in revised form 7 August 2025
Accepted 30 August 2025

Keywords:

No-Core shell model
Nuclear structure
Core polarization
Form factors
Electron scattering
Nuclei

ABSTRACT

The present paper calculates the energy levels and electron scattering form factors of several medium and light nuclei. This calculation involves many components that need to be taken into account to ensure both feasibility and accuracy, including mathematics methods, quantum mechanical theory, and the theoretical framework and formulas of the nuclear shell model. In this study, the energy levels of ^{6}Li nuclei were calculated using the no-core shell model with WBT, WBM, and WBP effective residual interactions. The core shell model was employed to calculate the energy levels for the ^{32}S and ^{92}Mo nuclei. Based on the no-core shell model energy level calculations, the theoretical elastic (C0) electron scattering form factors of ^{6}Li were obtained, while the core shell model was used to calculate the longitudinal C2 electron scattering form factor for the ^{32}S, ^{92}Mo, and ^{90}Zr nuclei using the Tassie Model (TM). Potentials of the SKX(Skyrm Interaction\ force) and HO (Harmonic Oscillator) were utilized calculate the radial single-particle matrix elements' wave functions. The Shell model code NuShell-X@MSU was utilized in this present work. The energy level calculations of the ^{6}Li nuclei with WBM and WBT interactions show good agreement with experimental data compared to the wbp interaction. The core shell model calculations for the energy levels of ^{32}S and ^{92}Mo nuclei show reasonable agreement with the experimental data. In addition, the longitudinal C2 inelastic electron scattering form factors of ^{92}Mo, ^{90}Zr, and ^{32}S nuclei exhibit good agreement with experimental results.

INTRODUCTION

In nuclear physics, the core and no-core shell model spaces denote distinct methodological approaches. In the core shell model a segment of the nucleus is treated as a fixed core, whereas the no-core shell model treats all nucleons as dynamic particles within the model space [1]. The primary challenge in the no-core shell model is the exponential expansion of the model space with increasing nucleon number, which makes rendering computations for nuclei computationally demanding.

The model of the Nuclear Shell provides a significant theoretical tool for understanding nuclear properties. In its simplest form, it can be used as an individual particle model to provide qualitative conceptions; however, it has been utilized as well, as a foundation for more complex and Comprehensive calculations. Despite its success, there appear to be limitations on the further expansion of its applications in the near future [1].

Electron scattering from nuclei provides significant information concerning electro-magnetic currents within nuclei. The electronic scattering is capable of providing sufficient tool for that computation due to the fact that it has sensitivity to the spatial distribution of current and charge densities. Significant data concerning nuclear structures may be produced from high energy electron scattering. The information obtained from high-energy electron scattering depends on the de Broglie wave-length of the incident electrons compared with the nuclear force range. When the energy of the incident electron is 100 MeV and higher, its de Broglie wave-length becomes

*Corresponding author.
E-mail address: ameen.a.mohaimeed81@gmail.com
DOI: https://doi.org/10.55981/aij.2026.1644

comparable to the spatial extent of the target nucleus. Consequently, electrons at these energy levels can be considered as a optimal probe for studying nuclear structure [2-4].

The electron scattering has been considered as the most significant tool for studying nuclear structures for several reasons. The interaction between nucleus and electron is commonly known to occur through electromagnetic interactions with local charge distributions, magnetic densities and current. Measurements can therefore be obtained with minimal impairment to the structure of target nucleus. In contrast, for nucleon-nucleus scatterings, neither the structure nor the interaction of target is sufficiently well known, making it highly challenging to differentiate these effects the analysis of experimental data. Electron scattering, however, allows the scattering cross section with components of the operators' transition matrix in the current density and local charge, which are thus directly linked to the nuclear structure of the target [5,6]. Electron scattering can be classified into 2 main types, In the first, the nucleus remains in its ground state; such procedure is referred to as the “Elastic Electron Scattering”. In the second, the nucleus is left in one of its excited states, such procedure is known as “Inelastic Electron Scattering” [7].

METHODS

Inelastic longitudinal form factor

These include angular momentum (J) and momentum transmission (q) [8] and may be expressed as reduced matrix elements in the angular momentum as well as the iso-spin Eq. (1).

$$\left|F_J^L(q)\right|^2 = \frac{4\pi}{Z^2(2J_i+1)}\left|\sum_{T=0,1}(-1)^{T_f-T_{zf}}\begin{pmatrix} T_f & T & T_i \\ -T_{Z_f} & 0 & T_{Z_i}\end{pmatrix}\left\langle f \left\| \hat{T}_{JT}^L(q) \right\| i\right\rangle\right|^2$$
$$|F_{cm}(q)|^2\,|F_{fs}(q)| \tag{1}$$

Longitudinal operator matrix’s Reduced elements in spin and iso-spin spaces provided between final and initial states, several system particles, which include configuration mix in the term of One-Body Density Matrix (OBDM) elements that are multiplied by elements of single particle matrix of longitudinal operators Eq. (2) [9], in other words,

$$\left\langle f \left\| \hat{T}_{JT}^L \right\| i\right\rangle = \sum_{a,b} OBDM^{JT}(i,f,J,a,b)\left\langle b \left\| \hat{T}_{JT}^L \right\| a\right\rangle \tag{2}$$

Elements of OBDM have been represented as iso-spin reduced elements of the matrix [10], in other words, Eq. (3).

$$OBDM(\tau_Z) = (-1)^{T_f-T_z}\begin{pmatrix} T_f & 0 & T_i \\ -T_Z & 0 & T_Z\end{pmatrix}\sqrt{2}\,\frac{OBDM(\Delta T=0)}{2}$$
$$+\tau_Z(-1)^{T_f-T_z}\begin{pmatrix} T_f & 1 & T_i \\ -T_Z & 0 & T_Z\end{pmatrix}\sqrt{6}\,\frac{OBDM(\Delta T=1)}{2} \tag{3}$$

Elements of OBDM have been represented as iso-spin reduced elements of the matrix [10], in other words, represent iso-spin operators of the single particle. OBDM(ΔT) described in the following form Eq. (4) [10].

$$OBDM(i,f,j,j',\Delta T) = \frac{\left\langle f \left\| \left[a_j^+ \times \tilde{a}_{j'}\right]^{J,\Delta T} \right\| i\right\rangle}{\sqrt{2J+1}\;\sqrt{2\Delta T+1}} \tag{4}$$

a_j^+ operator created nucleon in the single nucleon state j and $\tilde{a}_{j'}$ had annihilated nucleon in j' state.

Tassie Model (TM) was utilized for the characterization of transition of gamma- as well as nuclei excitation by the electrons scattering. Based on collective modes Eq. (5) [11], core polarization transition density represented by TM.

$$\rho_{Jt_z}^{core}(i,f,\mathrm{r}) = \mathrm{N}\,\frac{1}{2}(1+\tau_z)\,\mathrm{r}^{J-1}\,\frac{d\rho_o(i,f,\mathrm{r})}{d\mathrm{r}} \tag{5}$$

N denotes the constant of the proportionality and ρ_0 denotes ground state 2 - body charge distributions of density. Coulomb form factor for such model constant of proportionality N may be calculated from form factor Eq. (6) and Eq. (7) that has been assessed at $q=k$, which results in:

$$F_J^L(q) = \left(\frac{4\pi}{2J_i+1}\right)^{1/2}\frac{1}{Z}\left\{\int_0^\infty \mathrm{r}^2 j_J(q\mathrm{r})\,\rho_{Jt_z}^{ms}\,d\mathrm{r} - \mathrm{N}q\int_0^\infty d\mathrm{r}\,\mathrm{r}^{J+1}\rho_o(i,f,r)\,j_{J-1}(q\mathrm{r})\right\}$$
$$\mathrm{x}\; F_{cm}(q)\,F_{fs}(q) \tag{6}$$

Where

$$\mathrm{N} = \frac{\int_0^\infty d\mathrm{r}\,\mathrm{r}^2 j_J(k\mathrm{r})\,\rho_{Jt_Z}^{ms}(i,f,\mathrm{r}) - F_J^L(k)\,Z\sqrt{\frac{2J_i+1}{4\pi}}}{k\int_0^\infty d\mathrm{r}\,\mathrm{r}^{J+1}\rho_o(i,f,\mathrm{r})\,j_{J-1}(k\mathrm{r})} \tag{7}$$

RESULTS AND DISCUSSION

Levels of energy

Results The calculations in this study were performed using the shell model space code Nushellx@msu for Windows. The first and essential step was to calculate the energy levels and then calculate the electron scattering form factors. The energy level calculations of the 6Li nucleus were performed using the no-core (SPSDPF) model space; the core shell model space was used for the energy level calculations of 32S and 92Mo nuclei. Nuclear Structure Calculations of Some Nuclei, nuclear form factors for the ^{6}Li, ^{92}Mo, ^{90}Zr, and ^{32}S nuclei were calculated with the same code.

Figure 1 presents a comparison between our theoretical calculations and the experimental data for the positive and negative parity energy levels of the ^{6}Li nucleus, obtained using the no-core model space with the SPSDPF configuration of 1s1/2,1p3/2,1p1/2,1d5/2,1d3/2,2s1/2,1f7/2,1f5/2, 2P3/2, 2P1/2. Three effective residual interactions (WBT, WBM, and WBP) were employed. These interactions are commonly used within the no-core framework and represent different parameterizations of the nucleon-nucleon interaction, as well as different treatments of handling three-body forces [12].

The calculations indicate that the interactions of show good agreement with the experimental data compared with the interaction for energies below approximately 18 MeV. In Fig. 1, nuclear energy levels appear in the theoretical results that are not observed experimentally, namely the 1_1^- and 1_2^- states.

Figure 2 presents a comparison of the experimental and theoretical excited energy levels of the ^{32}S nucleus. We used the HASP Model Space [13,14] for our theoretical calculations. The HASP model space employs the 1d3/2, 2p3/2, 2s1/2, and 1f7/2 orbitals (Eq2). The HASP model space comprises a mixing of the configuration from the SD model space (2s1/2 and 1d3/2) (Eq2), and the FP model space (1f7/2 and 2p3/2) (Eq3). The results show sufficient agreement between the experimental values and the theoretical level. The difference between theoretical calculations and practical data on the excited energy levels of the ^{32}S nucleus was ranging from 0.25 to 1.2 MeV.

The energy levels of the ^{92}Mo nucleus were calculated using N50J model space, which includes configurations with nucleons occupying orbitals up to the N = 50 shell closure; its configurations are 2P3/2,1F5/2,2p1/2,1g9/2. (Eq4) Fig. 3 compares the calculated energy levels of ^{92}Mo nucleus with the experimental data [15,16]. The results show satisfactory agreement, with the results demonstrate satisfactory agreement, with differences between theoretical calculations and experimental values of less than 0.3 MeV.

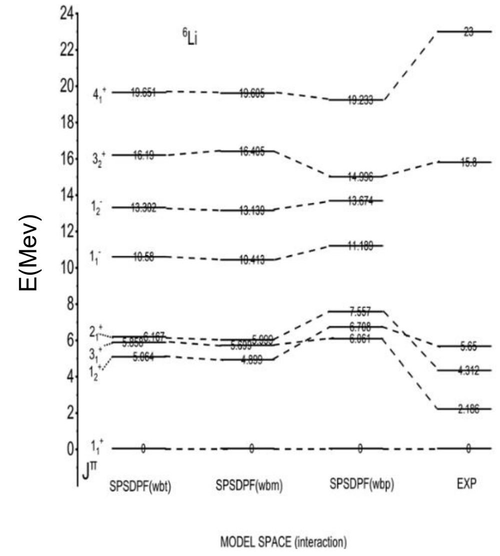

Fig. 1. Energy levels for ^{6}Li nuclei with no-core model space in comparison to the experimental data (EXP).

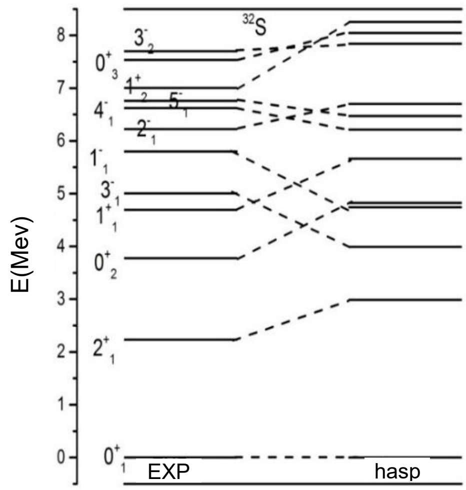

Fig. 2. The calculations of Energy levels (hasp) of ^{32}S nuclei in comparison to the experimental data (EXP) [15].

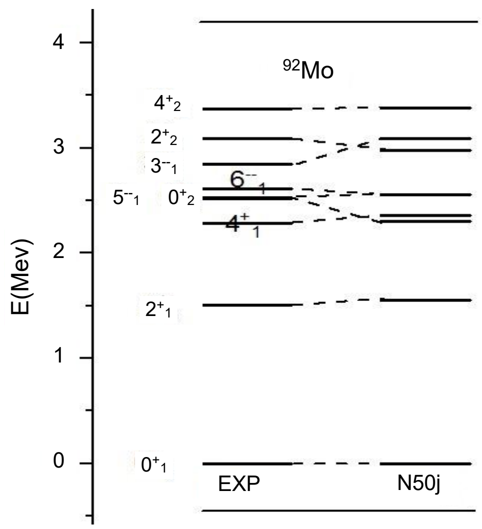

Fig. 3. The calculations of energy levels (n50j) of ^{92}Mo nuclei in comparison to the experimental data (EXP) [16].

Longitudinal electron scattering form factors

We calculated the longitudinal (Coulomb) components of electron scattering form factors for ^{92}Mo, ^{90}Zr, and ^{32}S nuclei by employing the core polarization using the Tassie Model (TM). Potentials of SKX (X = 20) and Harmonic Oscillator (HO) were employed to calculate the radial single-particle wave functions and their matrix elements. The inelastic longitudinal form factor for the C2 (2_1^+4) state of the ^{92}Mo nucleus was calculated using the SKX (dashed curve) and HO (solid curve) potentials, as represented in Fig. 4). The theoretical calculations showed good agreement with the experimental data at the first peak when the effective charge value of 0.50 was used. However, both two potentials showed insufficient agreement at the second peak. These calculations were carried out within the model space of N50J [17].

Figure 5 presents the calculations of the longitudinal C2 (2_1^+5) inelastic electron scattering form factors of the ^{90}Zr nucleus. The calculations were also carried out using the N50J interactions and the Tassie model with the SKX and HO potentials. The theoretical calculations show good agreement with experimental data at the 1st peak, whereas calculations with the SKX provides closer agreement to experimental results at the 2nd peak.

Longitudinal C2 form factors, including core-polarization effects (TM) for transitions to the (2_1^+0) in ^{32}S is illustrated in Fig. 6, in comparison to the experimental results. The theoretical calculations show good agreement with the experimental data at both the 1st and 2nd peak regions.

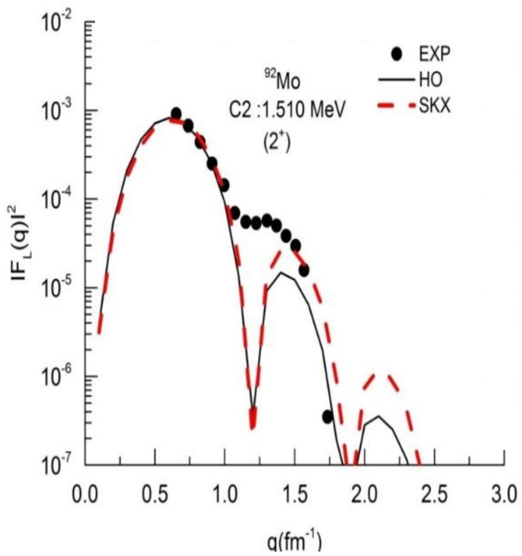

Fig. 4. The calculations of the C2 form factors (solid and dashed curves) for ^{92}Mo nuclei in comparison to their corresponding Experimental data (dotted curve) [18].

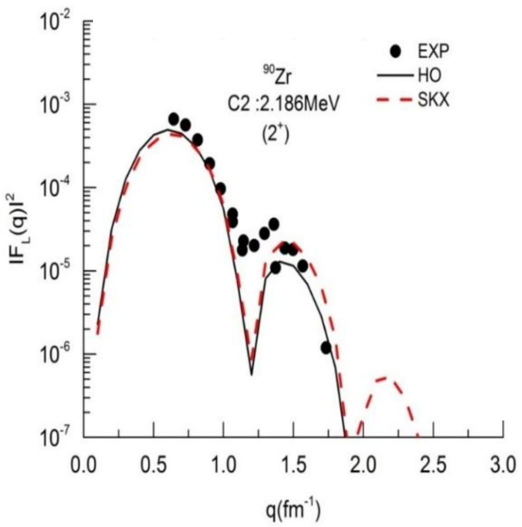

Fig. 5. The calculations of the C2 form factors (solid and dashed curves) for the ^{90}Zr nuclei in comparison to their corresponding Experimental data (dotted curve) [18].

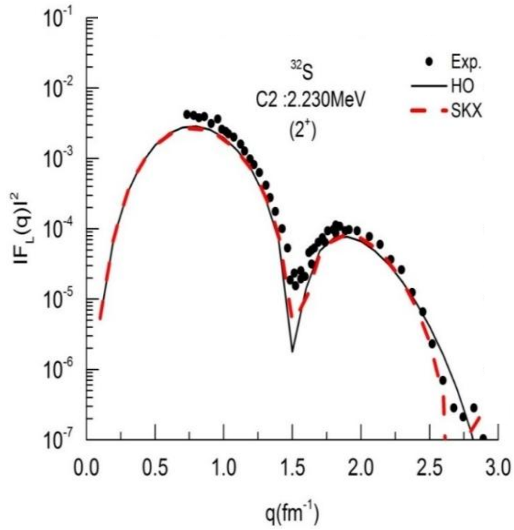

Fig. 6. The calculations of the C2 form factors (solid and dashed curves) in the ^{32}S nucleus compared to their corresponding Experimental data (dotted curve) [19,20].

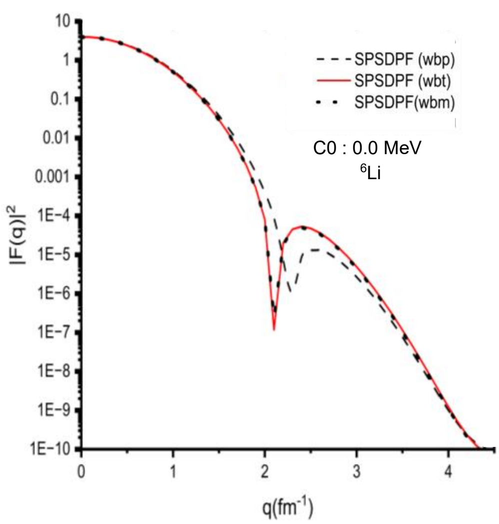

Fig. 7. The calculations (theoretical) elastic electron scattering form factors for ^{6}Li nuclei.

Figure 7 shows the theoretical elastic electron scattering form factors calculated within the plane wave Born approximation for the ^{6}Li nuclei. These calculations are based on the no-core model space of SPSDPF and employ the interactions of (solid curve), (dotted curve), and (dashed curve). A comparison with any experimental data was not provided due to the lack of available experimental measurements for the ^{6}Li nuclei.

CONCLUSION

The energy levels of ^{6}Li were calculated using the no-core shell model, which treats all nucleons in the nucleus as active. The no-core calculations employed three effective residual interactions. The calculations indicate that the interactions and give good agreement with experimental data compared to the interaction. Energy levels of the ^{32}S nucleus with the HASP model space have differences between theoretical calculations and experimental data ranging between 0.25 and 1.2 MeV. The energy levels of ^{92}Mo show that the agreement is satisfactory between the calculated and experimental data, where the differences between them are less than 0.3 MeV. The theoretical longitudinal C2 inelastic electron scattering form factors of the ^{92}Mo, ^{90}Zr, and ^{32}S nuclei give good agreement with experimental data. Theoretical calculations of the nuclear form factors for the ^{6}Li nucleus were performed based on the energy levels from the no-core shell model. Although no experimental data for the ^{6}Li form factors are available, the general form of the calculations is consistent with the standard form of elastic nuclear form factors.

ACKNOWLEDGMENT

The authors extend their thanks and appreciation to the Babylon Education Directorate and the Karbala Education Directorate for the facilities they provided to complete this research.

AUTHOR CONTRIBUTION

A. The author Ameen Alwan Mohaimeed wrote the main basics of the manuscript. The authors Shamil R. Sahib analyzed the data and the figures. All authors reviewed the manuscript.

REFERENCES

1. B. A. Brown, Nucl. Phys. A. **704** (2002) 11.
2. L. Lapikas, A. Dieperink, and G. Box, Nucl. Phys. A. **203** (1973) 609.
3. J. Bergstrom, S. Kowalski, and R. Neuhausen, Phys. Rev. C. **25** (1982) 1156.
4. R. R. Roy and B. P. Nigam, Nuclear Physics: Theory and Experiment, John Wiley & Sons, Inc., New York (1967).
5. H. Benson and B. Flowers, Nucl. Phys. A. **126** (1969) 305.
6. J. D. Walecka, Electron Scattering for Nuclear and Nucleon Structure, Cambridge University Press, Cambridge (2001).
7. D. J. Millener, D. Sober, H Crannell *et al.*, Phys. Rev. C. **39** (1989) 14.
8. T. W. Donnelly and I. Sick, Rev. Mod. Phys., **56** (1984) 461.
9. P. J. Brussaard, and P. W. M. Glaudemans, Shell-model applications in nuclear spectroscopy, North-Holland Publishing Company, Amsterdam (1977).
10. B. A. Brown, R. Radhi, and B. H. Wildenthal, Electric Quadrupole and Hexadecupole Nuclear Excitations from the Perspective of Electron Scattering and Modern Shell-Model Theory, North-Holland Publ. Co., Amsterdam (1983).
11. L. J. Tassie, Aust. J. Phys. **9** (1956) 407.
12. R. S. Abdullhussein, J. Tech. **4** (2022) 45.
13. J. Beene, Nucl. Data Sheets **25** (1978) 235.
14. M. Bissell, J. Papuga, H. Naïdja *et al.*, Phys. Rev. Lett. **113** (2014) 052502.
15. C. Ouellet and B. Singh, Nucl. Data Sheets **112** (2011) 2199.
16. C. M. Baglin, Nucl. Data Sheets **113** (2012) 2187.
17. X. Ji and B. Wildenthal, Phys. Rev. C. **40** (1989) 389.
18. P. X. Ho, J. Bellicard, P. Leconte *et al.*, Nucl. Phys. A. **210** (1973) 189.
19. B. H. Wildenthal, B. A. Brown, and I. Sick, Phys. Rev. C. **32** (1985) 2185.
20. A. M. Haifani, W. Prakoso, T. Setiadipura *et al.*, Atom Indones. **52** (2026) 29.